Sequential processing from cell lysis to protein assay on a chip enabling the optimization of an F_1-ATPase single molecule assay condition†

Tetsuya Nakayama,[a] Moriaki Namura,[a] Kazuhito V. Tabata,[b] Hiroyuki Noji[b] and Ryuji Yokokawa*[cd]

Received 9th June 2009, Accepted 14th September 2009
First published as an Advance Article on the web 13th October 2009
DOI: 10.1039/b911148d

We developed an integrated protein assay device, "Single Molecule MicroTAS (SMM)," which enables cell lysis, protein extraction, purification, and activity assay. The assay was achieved at the single-molecule scale for a genetically engineered protein, F_1-ATPase, which is the smallest known rotary motor. A cell lysis condition, with a wide range of applied voltages (50–250 V) and other optimized values (pulse width: 50 μs; duty: 0.01%; electrode gap: 25 μm; total flow rate: 5 μL min^{-1}) provided a high enough protein concentration for the assay. Successively, the protein was extracted and purified by specific binding in a microfluidic channel. During the assay process, the diffusion effect of lysate between a two-phase laminar flow contributes to optimizing the single-molecule assay condition, because the concentration of the original lysate from the *E. coli* solution is too high to assay. To achieve the most efficient assay condition, the protein diffusion effect on the assay was experimentally and numerically evaluated. The results reveal that, in our experimental conditions, concentrations of F_1 and other contaminated effluents are optimized for the F_1 rotational assay at a channel position. The adenosine triphosphate (ATP)-driven rotation speed measured in the SMM was compatible with that obtained by conventional purification and assay. Such a sequential process from cell lysis to assay proves that the SMM is an example of a sample-in-answer-out system for F_1 protein evaluation.

Introduction

Traditionally, Micro Total Analysis Systems (MicroTAS) developed miniaturized bulk scale processes for the analytical chemistry field. Recently, MicroTAS researchers have focused on the miniaturization of biochemical processes for genetic engineering applications. Essential components, such as cell transformation by injecting plasmid deoxyribonucleic acid (DNA), cell culture, cell lysis, and biomolecule detection, have been demonstrated on a microfluidic chip.[1–4] Moreover, some groups realized their integration of sequential processing: cell lysis to the polymerase chain reaction (PCR) of extracted DNA, cell lysis to the fluorescent detection of eluted proteins.[5–7] However, such MicroTAS still needs to integrate more components to eliminate off-chip processing, resulting in a more simplified sample-in-answer-out system. The integration mostly faces difficulties in handling the different sample concentrations demanded in each process, *e.g.* purified biomaterials often need to be concentrated for the subsequent detection step. This is because researchers try to simply downscale bulk scale experiments in genetic engineering to on-chip processing at the micrometer-scale. Though concentration and dilution devices are necessary between processes,[8,9] their integration is still not well achieved. Therefore, the next stage is to sequentially integrate multiple processes on a chip, such as injecting a few microlitres of cell solution, cell lysis, extraction of target protein and DNA, and their quantitative or activity measurement.[10]

To address difficulties in the integration of sequential processes, we focus on a single molecule assay of proteins extracted from cells. Traditionally, experiments to elucidate behaviour of a molecule have been termed single molecule assay or analysis, even though those protein molecules are numerous in an assay condition.[11–14] This approach realizes the protein activity measurement at the single molecule level without concentration or dilution processes. Activities of single molecules, such as myosin,[15] kinesin,[16–18] F_1-ATPase,[19] DNA and ribonucleic acid (RNA) polymerase,[20] β-galactosidase[21] have been evaluated from a scientific point of view. Such single molecule analysis offers great opportunities in drug screening to reveal a relationship between molecules and diseases, because some of them are known to affect cell functions.[14,22]

In most conventional biochemical analysis, the activity of a single molecule has been measured by dividing the average activity obtained on the bulk scale by the number of molecules in the solution. However, when we are able to measure the activity of a single molecule directly, it is no longer necessary to determine the concentration of target molecules. Our ultimate goal is to extract target molecules from a single cell and evaluate one of them by taking advantage of single molecule analysis. It will provide a universal MicroTAS, which has the capabilities of evaluating plasmid DNA and genetically

[a]*Graduate School of Science and Engineering, Ritsumeikan University, 1-1-1 Noji-Higashi, Kusatsu, Shiga, 525-8577, Japan*
[b]*The Institute of Scientific and Industrial Research (ISIR), Osaka University, 8-1 Mihogaoka, Ibaraki, Osaka, 567-0047, Japan*
[c]*Department of Microengineering, Kyoto University, Yoshida-honmachi, Sakyo-ku, Kyoto, 606-8501, Japan. E-mail: ryuji@me.kyoto-u.ac.jp; Fax: +81 75 753 3559; Tel: +81 75 753 3559*
[d]*PRESTO/CREST JST, 4-1-8, Hon-chou, Kawaguchi, Saitama, 332-0012, Japan*

† Electronic supplementary information (ESI) available: 1. Cell lysis evaluation by SDS-PAGE. 2. The on-chip rotation assay using pseudo-lysates. See DOI: 10.1039/b911148d

engineered protein, essential in genetic engineering processes. By choosing one well-studied motor protein, the F_1-ATPase (hereafter F_1, known as the F_1 moiety of the F_oF_1-ATPsynthase) as a target protein molecule, we developed a "Single Molecule MicroTAS (SMM)," in which the protein extracted from *Escherichia coli* (*E. coli*) cells is purified and evaluated at the single-molecule level. To ensure compatibility of our on-chip assay with benchtop assay, we evaluated on-chip functions by measuring *E. coli* and protein concentrations throughout experiments.

The device was designed specifically for a genetically modified strain of *E. coli*, which expresses a large number of F_1 molecules. The device can be applied simply to other kinds of single molecule studies, including motor proteins. It will accelerate understanding of molecular functions because many chemical reactions can be detected only by focusing on countable number of molecules, even single molecules. Moreover, the molecular analysis using a micro/nano fabricated structure is more advantageous than that using only a conventional flow cell.[23] In contrast, a substantial amount of molecules is still necessary to reveal biological processes. It is not a step in the right direction to stack multiple SMM to increase the number of analyzing molecules for such purposes. We yield those assay conditions to other MicroTAS developed for cell level analysis.[24,25]

Essential components in such a SMM can be divided into two parts: one is the cell lysis part to extract DNA and protein, and the other is their purification and assay at the single-molecule level. Many on-chip cell lysis methods have been reported using physical,[26,27] chemical,[6,28] thermal,[7] and electrical[29,30] damage on cells. Almost all methods are developed for DNA extraction and evaluation, causing denaturing of proteins, especially, chemical and thermal cell lysis denatures, and severely deactivates proteins. To retrieve both DNA and protein, physical or electrical methods are preferable. However, applying physical damage on the cells demands relatively large structures, such as a piezoelectric vibration mechanism[27] or nano-scale edge structures.[26] For future integration in the SMM, our first prototype utilizes a high electric field between microelectrodes.[30,31] We also note that it is advantageous to use *E. coli* cells, which are frequently used in the genetic engineering field, because they can be lysed relatively easily, compared with other kinds of cells.[26–28,32]

The other part, purification and assay of a target molecule, was usually processed separately for DNA and protein. DNA molecules are so stable that they are first captured on microspheres or silicon substrates, and eluted for their evaluation.[28,33,34] On the other hand, protein molecules have to retain three-dimensional structures to express their functionalities in the assay. Normally, the on-chip capillary electrophoresis separates and purifies the proteins depending on molecular weight, allowing us to identify proteins and to determine their concentrations.[35–37] However, such processing mostly results in the denaturation of proteins as a result of surfactants. Since it is necessary to detect not only protein existence but also its activity, we adopted a specific molecular binding between His-tag and nickel-nitrilotriacetic acid (Ni-NTA) to separate the target F_1 from other intracellular materials. Another binding between biotin and streptavidin was also utilized for its single molecule assay.

Experimental

Device fabrication

The SMM shown in Fig. 1(a) has sequential functions, such as cell lysis, protein dilution by laminar flow, purification, and assay. The device consists of the bottom coverslip and the top polydimethylsiloxane (PDMS) channel structure. The coverslip has patterned chromium/gold (Cr/Au) electrodes for cell lysis and a Ni-NTA coating for F_1 purification (Fig. 1(b)). The top PDMS layer provides microfluidic channels with two inlets and one outlet, as shown in Fig. 1(c). One of the inlets used for *E. coli* cell injection is connected to the cell lysis chamber, and the other is utilized for introducing dilution buffer solutions. The following paragraphs describe the detailed processes.

A coverslip (24 mm × 36 mm, No. 1: 0.12–0.17 mm thick, Matsunami) was washed in a 10 M KOH solution. On the coverslip, Cr and Au layers were thermally evaporated (VPC-260F, ULVAC, Inc.) to thicknesses of 10 nm and 140 nm, respectively. Positive photoresist (OFPR-800 LB 54 cp, Tokyo Ohka Kogyo Co., Ltd.) was spin-coated and patterned as a mask layer for the Cr/Au etching. The Au layer was first removed using a potassium iodide–iodine solution (KI : I_2 : deionized water (DIW) = 4 : 1 : 80, mass ratio), followed by Cr layer etching. Acetone and ethanol cleaned the patterned photoresist mask. Using an emulsion mask, the narrowest gap of 25 μm was obtained between the triangular-shaped electrodes in a parallel array. Masking the patterned electrodes by a PDMS slab, Ni-NTA was coated on the assay area only for the specific capturing of F_1. The coverslip was first immersed in 1 mM CH_3COOH solution, and then 2% 3-mercaptopropyltrimethoxysilane (LS-1390, Shin-Etsu Chemical Co., Ltd.) and 0.8% ethanol were added to the solution. After 1 h incubation at room temperature, the coverslip was washed by DIW and heated on a hotplate (120 °C, 1 h) for tight coupling of the silane and glass surfaces. The coverslip was sequentially immersed in

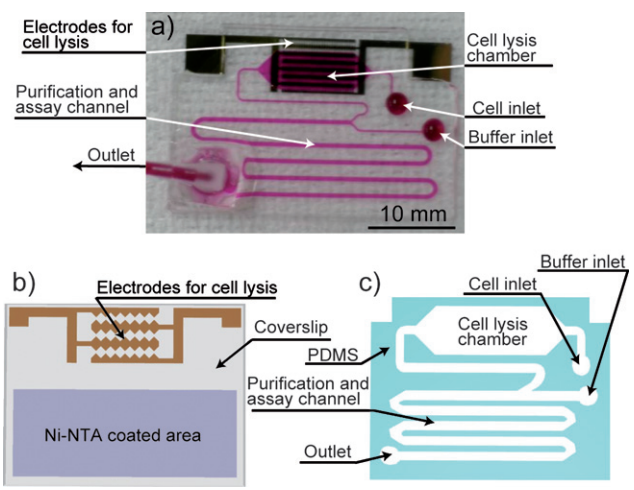

Fig. 1 A Single Molecule MicroTAS (SMM) integrating cell lysis, protein extraction–purification–assay components: (a) A SMM overview. Microfluidic channels are coloured by red ink for clarity. The bottom glass coverslip (b) has patterned Au electrodes and Ni^{2+}-NTA coatings in the purification and assay channel region. The top PDMS channel structure (c) is prepared by a standard moulding process.

a dithiothreitol solution (1 mM DTT in DIW) for 30 min, a maleimide solution (5 mg mL^{-1} maleimido-C3-NTA (345–90711, Dojindo Laboratories), 50 mM MOPS-KOH (pH 7.0), 50 mM KCl) for 1 h, and a Ni^{2+} solution (10 mM $NiSO_4$ in DIW) for 30 min, along with washing by DIW after each incubation. The PDMS slab for masking was removed and the coverslip surface thoroughly washed by DIW.

A standard moulding process prepared the top PDMS layer. The master for the PDMS replica was prepared by patterning a thick photoresist SU-8 3050 (MicroChem Corp.) on a silicon wafer. The PDMS prepolymer and curing agent (Silpot184W/C, Dow Corning Toray Co., Ltd.) were mixed at a ratio of 10 : 1 and poured onto the silicon mould. Following the curing process at 90 °C for 1 h, the slab was removed from the mould. Dimensions for the cell lysis chamber and assay channel were $D = 150$ μm, $W = 5$ mm, $L = 11$ mm, and $D = 150$ μm, $W = 580$ μm, $L = 120$ mm, respectively. The PDMS replica was bonded directly onto the cleaned coverslip, and two inlet and outlet holes punched for connections to syringe pumps (IC3210, KD Scientific Inc.).

Sample preparation

The *E. coli* strain used in our experiment, JM103 Δ(*unc*B-*unc*D), was genetically engineered to express the mutant complexes of F_1 from the thermophilic *Bacillus* PS3.[38] For this gene expression, a plasmid pKAGB1 carried F_1 mutant genes for the α(C193S and 6 His-tag at N terminus), γ(S107C/I210C), and β(10 His-tag at N terminus).[39] The F_1 mutant was purified according to the method of Noji *et al.*[40] The transformed *E. coli* cells were cultured using a LB agar plate and 35 mL medium, including 0.1 mg mL^{-1} ampicillin. The initial cell concentration for injecting the cell inlet was adjusted to 4×10^8 cells mL^{-1}. This was achieved by defining a correlation between cell concentration and absorbance OD_{600} (UV-1700, Shimadzu Corp.).

As a control experiment to the sequential assay on SMM, we separately purified an F_1 off-chip using the same construct as described above. Cells were cultured up to 1 L Luria Broth (LB) medium and collected by conventional centrifugation steps. Cell lysate obtained by sonication was injected into an affinity column filled with Ni-NTA Agarose beads (30210, Qiagen, Valencia, CA). F_1 fusing 6 × His-tagged proteins were eluted by imidazole. The eluate was desalted by a prepacked disposable column (PD-10, 17-0851-01, GE Healthcare), resulting in a final F_1 concentration of about 2.5 μM.

For the off-chip ATP-driven rotation assay, we prepared a 5 mm × 20 mm flow chamber using a Ni-NTA-coated coverslip, and a non-coated one with spacers. The purified F_1 molecules, diluted to 0.2 nM in a buffer A (50 mM MOPS-KOH (pH 7.0), 50 mM KCl, 2 mM $MgCl_2$) were immobilized by His-tags and Ni-NTA bindings. Streptavidin-coated microspheres (~0.68 μm in diameter, Seradyn, Inc.) were attached to the biotinylated γ-subunit. Finally, 2.5 mM ATP in a buffer B (2 mg mL^{-1} BSA in Buffer A) was injected to initiate F_1 rotations recognized by the microsphere rotation. The bead rotation was observed using an inverted microscope with a 100× oil-immersion objective (IX71, Olympus Corp.) and captured by CCD camera (WAT-120N, Watec Co., Ltd.) at the video rate. After conversion to an AVI file, the rotation speed was analysed using PC-based software (Image J, NIH).

Sequential assay

The sequential processing in the SMM from the cell lysis to the single molecule assay was performed by the liquid manipulation, as listed in Table 1. Before starting the process, DIW filled the fluidic system, and was then replaced by buffer A to avoid bubble formation inside channels. The flow rate was kept at 5 μL min^{-1} throughout the process by sucking at the outlet. A cell suspension of 4 μL was injected and lysed by applying a pulse voltage for 10 min, which was long enough to immobilize eluted F_1 on the Ni-NTA-coated channel surface and to remove cell debris from the assay channel. A function generator (WF1943B, NF) and a bipolar amplifier (HSA4052, NF) applied the electric field. For protein purification by removing contaminated proteins and a blocking of glass surface for the following assay, buffer A and B were sequentially introduced for washing for 20 min in total. The streptavidin-coated microspheres in buffer B were immobilized on the biotinylated γ-subunit in a flow chamber. After this process, the buffer solution was incubated for 10 min without syringe manipulation, resulting in a higher yield of avidin–biotin bindings. Refer to the schematic illustration in Fig. 4(b) for these molecular bindings. Following the washing of microspheres by buffer B, a 2.5 mM ATP solution was introduced. The on-chip ATP-driven rotation assay was observed and analysed by the same experimental procedure described for the off-chip assay. The following experiments investigated the cell lysis and assay in detail.

The cell lysis efficiency was evaluated by recovering cell lysate at the downstream of the cell lysis chamber. The supernatant of the centrifuged (15 000 rpm, 4 °C, 20 min) lysate was analysed by absorptiometry OD_{280}. The absorbance was measured for solutions obtained by different cell lysis conditions: square pulse width (0–50 μs), applying different voltages (0–250 V, 0–100 kV cm^{-1})

Table 1 Assay protocol for the sequential assay in the SMM

	Cell inlet		Buffer inlet	
Process	Solution	Flow rate/μL min^{-1}	Solution	Flow rate/μL min^{-1}
Initialization	DIW	5.0	DIW	0.0
Cell lysis	Cell solution	3.0	Buffer A	2.0
Purification	Buffer A	3.0	Buffer A	2.0
Washing	Buffer B	2.5	Buffer B	2.5
	Bead solution	2.5	Bead solution	2.5
Single molecule assay	Incubation, 10 min			
	Buffer B	2.5	Buffer B	2.5
	ATP solution	2.5	ATP solution	2.5

and flow rates (1–10 μL min^{-1}). When one of the three parameters was varied, the other two were kept constant as follows: pulse width (50 μs), voltage applied (250 V, 100 kV cm^{-1}), and flow rate (3 μL min^{-1}). Pulse duty (0.01%) and the initial cell concentration were kept constant for comparison.

When eluted protein diffuse in the laminar flow during cell lysis and protein purification processes, a biased flow rate of 3.0 μL min^{-1} for the cell inlet and 2.0 μL min^{-1} for the buffer inlet were utilized to induce wider F_1 molecule distribution in the assay channel. The diffusion direction perpendicular to the buffer flow corresponded to the *y*-axis in the next numerical simulation section (see Fig. 5(a) for the coordinates). Once the single molecule assay system was established by bead injection, the number of rotating beads was counted in the assay channel. The bead density was averaged for each 50 μm channel width. Because of its dependency on the concentration of eluted proteins, we varied the applied voltage from 0 to 250 V. The other lysates obtained by off-chip sonication were also injected for comparison with on-chip cell lysis.

Numerical simulation for F_1-ATPase diffusion

During the cell lysis and protein purification processes, F_1 and contaminated intracellular materials diffuse in the *y*-direction at the downstream of the mixing point, where the cell lysate from the cell lysis chamber and buffer A merge. When two solutions are evenly mixed and generate a developed laminar flow, molecule diffusion can be estimated easily using an analytical solution for the one-dimensional diffusion equation. However, since the two flow rates were not equal, numerical simulation provided a more accurate diffusion profile for the target protein. Therefore, the profile was numerically calculated using a three-dimensional laminar flow model with the PC-based software, FLUENT 6.3. It is especially the case that the molecule distribution is not uniform in the *z*-direction, but is enhanced near the channel surface. This is because flow velocity is lower at the channel surface than in the middle of the channel, and is known as 'the butterfly effect'.[41,42] Therefore, to discuss assay efficiency, we focused on the F_1 density only on the channel surface. Table 2 lists the boundary conditions for the simulation. A diffusion coefficient of 25 μm^2 s^{-1} was used based on the Stokes–Einstein relationship by assuming an F_1 dimension of 10 nm, which is close to a protein with similar molecular weight.[6]

Results and discussion

Cell lysis and sequential assay

The behaviour of the *E. coli* cells during cell lysis was observed, as shown in Fig. 2. Even with a constant flow of 5 μL min^{-1} at the outlet, cells formed multiple pearl chains between the tips of the triangular-shaped electrodes. Therefore, eluted proteins, mostly F_1 molecules, flowed downstream for the rotation assay. The total amount of eluted proteins increased with an increase in applied voltage and pulse width and with decreasing of flow rates, as shown in Fig. 3(a)–(c). Here, we would like to note that F_1 is dominant compared with other contaminated proteins (see ESI,† 1. Cell lysis evaluation by SDS-PAGE). The result shown in Fig. 3(a) reveals that a longer exposure of *E. coli* cells to a dc electric field is preferable for effective cell lysis. Similar results were also reported for other kinds of cells.[43,44] We fixed the pulse width at 50 μs and evaluated the effects of field strength and flow rate. As expected, a higher electric field yields higher protein concentrations, as shown in Fig. 3(b). Fig. 3(c) implies that proteins are eluted, even with high flow rates, because a higher OD_{280} was measured than $OD_{280} = 0.027$ without any applied voltage. This is advantageous for the high throughput processing of target proteins. Focusing only on the amount of eluted protein, we can conclude that applying a higher voltage with a narrower electrode gap, lower flow rate, and longer pulse width are effective in the cell lysis. However, because of steric hindrance, higher F_1 concentration is not necessarily preferable for the single-molecule assay. This is usually performed with the F_1 concentration in the nM range, as mentioned for the off-chip assay. In addition, the flow rate should be kept high enough to provide a tolerable amount of time for the total process. Electrolysis was another problem caused by high voltage and long pulse width. Therefore, we chose the parameters based on this trade-off as follows: voltage applied (250 V), flow rate for the cell lysis chamber (3 μL min^{-1}), and pulse width (50 μs).

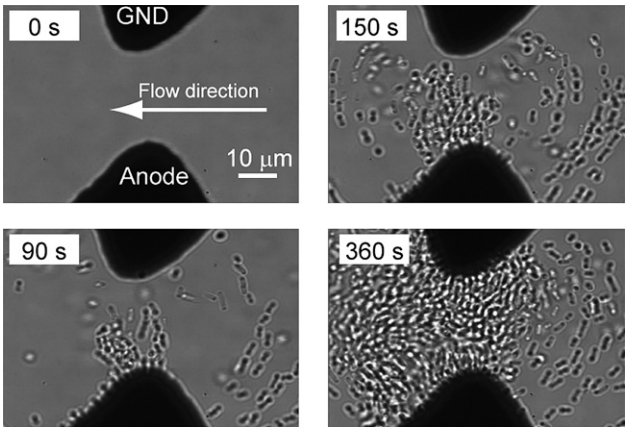

Fig. 2 *E. coli* cell lysis between a set of triangular electrodes.

The rotation of microspheres in the on-chip ATP-driven assay was captured with a frame rate of 15 fps, as shown in Fig. 4(a). For clarity, sequential images were taken of an F_1 motor protein with two microspheres, which was occasionally constructed by their aggregation. The molecular configuration is illustrated in Fig. 4(b). Rotations of a single microsphere could be still analysed because the γ-subunit did not bind to the centre of a microsphere given its ellipsoidal shape. We chose three rotating microspheres to analyse their rotation speed, as shown in Fig. 4(c). An average rotation speed of 1.8–3.1 rps for the on-chip assay is compatible with that of 1.9–2.6 rps for the off-chip conventional assay. The result implies that our SMM could

Table 2 Parameters for the numerical simulation of the F_1 concentration

Channel width for protein and buffer inlets	348 μm
Channel width for assay channel	580 μm
Channel height	150 μm
Flow rate for protein inlet	3 μL min^{-1}
Flow rate for buffer inlet	2 μL min^{-1}
Diffusion coefficient	25 μm^2 s^{-1}

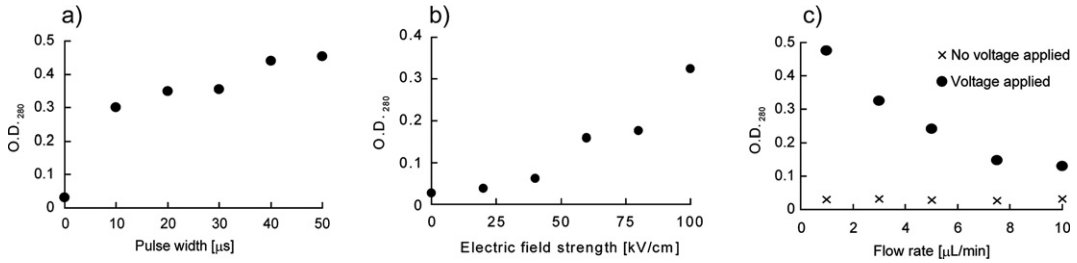

Fig. 3 Absorptiometry results of the cell lysis component in the SMM. The graphs show absorbance (OD_{280}) against (a) pulse width, (b) electric field strength, and (c) flow rate. The absorbance represents the concentration of eluted proteins.

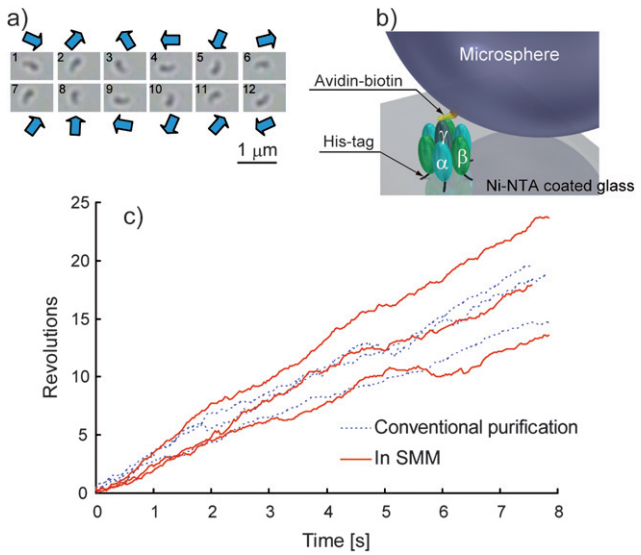

Fig. 4 (a) The ATP-driven F_1 rotation assay visualized by two aggregated microspheres. A frame rate of 15 fps was used to capture the sequential images. (b) Schematic illustration of protein configuration for the assay. (c) Comparison of the F_1 rotating speeds. Results obtained in the integrated device (SMM) and in the conventional assay using F_1 purified by benchtop purification are shown by solid red lines and dotted blue lines, respectively.

process from the cell lysis to the single molecule assay, which was also realized by benchtop protein purification and assay.

F_1 molecule diffusion

Fig. 5(a) shows the contour map for the F_1 molecule diffusion profile on the surface of assay channel. The normalized F_1 concentrations for one inlet (protein inlet) and the other (buffer inlet) were set to 1 (red) and 0 (blue), respectively. As designed, in shown in Fig. 1, the outlet is located at the channel downstream,

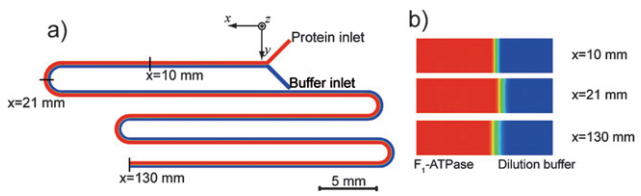

Fig. 5 (a) Contour map for F_1 molecules at the channel surface. Normalized F_1 concentration is coloured as red for 1 and blue for 0. (b) Concentration profiles for cross-sections at $x = 10$, 21, 130 mm.

$x = 130$ mm. The concentration profiles for cross-sections are shown in Fig. 5(b), depending on the position ($x = 10$, 21, 130 mm) in the flow direction. Comparing with a conventional laminar flow using the same flow rate for both inlets, the protein is widely dispersed to the buffer inlet side because of the biased flow rate (3 : 2) at the Y-junction. In particular, the dispersion at the channel surface is larger than that at the middle of the channel, given the butterfly effect.[41,42] We expected that this protein gradient would produce the best concentration for the single-molecule assay. To examine this assumption, we analysed the different assay conditions and compared them with the result from the numerical simulation.

The sequential assays in SMM were performed by applying six different voltages (0, 50, 100, 150, 200, 250 V) while keeping other parameters constant: the flow rate is listed in Table 1 and a pulse width of 50 μs was used. Therefore, the initial protein concentration flowing into the Y-junction varied depending on the voltage applied. In addition to these on-chip cell lysis, lysate obtained by off-chip sonication was also injected in to the SMM as a reference assay. For the numerical simulation results, the concentrations were normalized by $OD_{280} = 0.32$, measured at the applied voltage of 250 V corresponding to 100 kV cm^{-1} in Fig. 3(b). The computed F_1 concentrations in the y-direction are plotted, as shown in Fig. 6(a), where the results were averaged from the Y-junction ($x = 0$) to the outlet ($x = 130$ mm). For the y-axis, $y = 0$ and 580 μm correspond to the sidewalls in the assay channel of the F_1 protein and buffer inlet sides, respectively. The concentration gradient for the F_1 molecule is generated between $y = 300$ μm and $y = 400$ μm, though the initial concentration dominates $y = 0$–300 μm. Since the lysate prepared by sonication has a very high protein concentration of $OD_{280} = 11.5$, the gradient was plotted for $y = 380$–580 μm only.

Fig. 6(b) shows the corresponding experimental results. The densities of the rotating microspheres were plotted in the y-direction. They were measured throughout the channel ($x = 0$–130 mm) and averaged for each 50 μm width in the y-direction resulting in 11 data points. Cell lysates were obtained by the same conditions as above for Fig. 6(a): applying voltages of 0, 50, 100, 150, 200, 250 V, and off-chip sonication. Arrows indicate the positions where the highest density was obtained, which means that the assay condition for the F_1 molecule was optimized there. The same coloured arrows for the numerical simulation results in Fig. 6(a) point to the corresponding positions in the y-direction.

Comparing Fig. 6(a) and (b), we are able to expect to determine the F_1 concentration at a given cell lysis condition, which provides F_1 with the best condition to establish the molecular system for the single molecule assay. However, the F_1

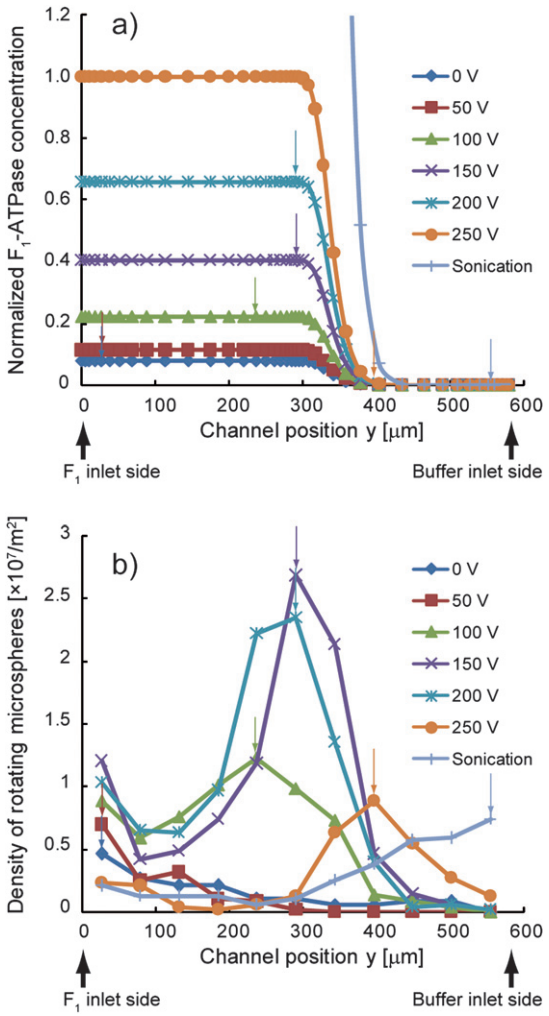

Fig. 6 (a) F_1 concentration in the *y*-direction channel depending on applied voltages for cell lysis. Concentrations are normalized by $OD_{280} = 0.32$ obtained at 250 V, and calculated results are averaged in the *x*-direction. (b) Density of rotating beads measured in the SMM. Arrows in (b) indicate the position where the highest density is obtained, and the corresponding *x*-positions are indicated in (a).

concentrations that yielded the highest densities for rotating microspheres in each cell lysis condition spread in a range from almost 0 to 0.65 in normalized concentration values in Fig. 6(a). The range is too wide to conclude that the F_1 concentration is optimized. This reveals that the assay condition was not optimized only with respect to the F_1 concentration but also to other conditions, including contaminants. This is because the molecular system for the rotation assay is established by layering Ni-NTA on the channel surface, the F_1 molecules, and a microsphere to the biotinylated γ-subunit. Such multilayer protein bindings cannot be explained by the target protein concentration only. F_1 molecules are mixed with other contaminated proteins and cell debris, and their diffusion coefficients range widely, depending on their size. The concentration ratio among these materials in lysate varies in the *y*-direction in the channel due to their different diffusion coefficients. Given the tug-of-war between the molecules in access to the channel surface (in other words the different binding affinities of molecules to the surface) the density of F_1 molecules bound to the Ni-NTA-coated glass surface may have a gradient in the *y*-direction. Assuming such a tug-of-war effect, the density of the rotating microspheres are maximized at a certain position with each given cell lysis condition.

Two factors support the tug-of-war effect: one is by comparison with a conventional off-chip assay condition, and the other is by an additional experiment mimicking the lysate dilution in a Y-shaped channel. In the off-chip assay using F_1 molecules, which is purified by a benchtop conventional protocol yielding a more highly purified protein than our SMM, the rotation assay cannot be observed at too high or too low a concentration. Too high a concentration causes steric hindrance among molecules, and too low a concentration decreases the probability of establishing the assay system due to its stochastic phenomenon (Fig. 4(b)). As stated in the off-chip experiment section, the nanomolar range is appropriate for observing the assay. As the second support, the additional experiment was performed to eliminate the possibility of a missed operation disturbing the protein concentration gradient in the SMM. Three kinds of pseudo-lysates were prepared and assayed in a simple Y-shaped channel. The density of the rotating microspheres had the same distribution as Fig. 6(b), where the highest efficiency was obtained at a certain position in the *y*-direciton (see ESI,† 2. The on-chip rotation assay using pseudo-lysates). Considering the above-mentioned issues, not only was the F_1 concentration optimized but all the assay conditions were too.

Conclusion

We have fabricated a "Single Molecule MicroTAS (SMM)," which comprises cell lysis, protein extraction, purification, and activity assay. Evaluating the cell function, we found that protein extraction by applying a pulse voltage is enough to achieve the single-molecule assay. The resulting F_1 rotation assay in the SMM is comparable with the off-chip conventional assay in which the concentration of the F_1 molecule is clearly optimized after purification by a laborious benchtop process. Considering the numerical simulation for the F_1 molecule diffusion and the experimental results for the rotation assay, we conclude that the SMM always optimizes the assay condition. Therefore, the molecular system for the single-molecule assay can be constructed with a given sample condition, *i.e.*, regardless of the cell initial concentration or the cell lysis condition. We expect the result to shed light on a new applicability of MicroTAS to single molecule evaluations.

Acknowledgements

This research was funded by PRESTO and CREST from Japan Science and Technology Agency (JST). The authors thank Prof. Y. Ogami and Dr Thien X. Dinhy of the Dept. of Mechanical Engineering, Ritsumeikan University for the supporting FLUENT software operation.

Notes and references

1 Y. S. Shin, K. Cho, J. K. Kim, S. H. Lim, C. H. Park, K. B. Lee, Y. Park, C. Chung, D. C. Han and J. K. Chang, *Anal. Chem.*, 2004, **76**, 7045–7052.

2 Y.-C. Lin, C.-M. Jen, M.-Y. Huang, C.-Y. Wu and X.-Z. Lin, *Sens. Actuators, B*, 2001, **79**, 137–143.
3 S.-W. Lee and Y.-C. Tai, *Sens. Actuators, A*, 1999, **73**, 74–79.
4 K. Sato, M. Tokeshi, T. Odake, H. Kimura, T. Ooi, M. Nakao and T. Kitamori, *Anal. Chem.*, 2000, **72**, 1144–1147.
5 J. Gao, X. F. Yin and Z. L. Fang, *Lab Chip*, 2004, **4**, 47–52.
6 E. A. Schilling, A. E. Kamholz and P. Yager, *Anal. Chem.*, 2002, **74**, 1798–1804.
7 C.-Y. Lee, G.-B. Lee, J.-L. Lin, F.-C. Huang and C.-S. Liao, *J. Micromech. Microeng.*, 2005, **15**, 1215–1223.
8 P. K. Wong, C. Y. Chen, T. H. Wang and C. M. Ho, *Anal. Chem.*, 2004, **76**, 6908–6914.
9 M. Yamada, T. Hirano, M. Yasuda and M. Seki, *Lab Chip*, 2006, **6**, 179–184.
10 S. J. Lee and S. Y. Lee, *Appl. Microbiol. Biotechnol.*, 2004, **64**, 289–299.
11 K. Svoboda, P. P. Mitra and S. M. Block, *Proc. Natl. Acad. Sci. U. S. A.*, 1994, **91**, 11782–11786.
12 A. D. Mehta, R. S. Rock, M. Rief, J. A. Spudich, M. S. Mooseker and R. E. Cheney, *Nature*, 1999, **400**, 590–593.
13 D. S. Friedman and R. D. Vale, *Nat. Cell Biol.*, 1999, **1**, 293–297.
14 F. Hong and D. D. Root, *Drug Discovery Today*, 2006, **11**, 640–645.
15 K. Kitamura, M. Tokunaga, A. H. Iwane and T. Yanagida, *Nature*, 1999, **397**, 129–134.
16 R. D. Vale, T. S. Reese and M. P. Sheetz, *Cell*, 1985, **42**, 39–50.
17 J. Howard, A. J. Hudspeth and R. D. Vale, *Nature*, 1989, **342**, 154–158.
18 S. M. Block, L. S. Goldstein and B. J. Schnapp, *Nature*, 1990, **348**, 348–352.
19 H. Noji, R. Yasuda, M. Yoshida and K. Kinosita, Jr., *Nature*, 1997, **386**, 299–302.
20 Y. Harada, O. Ohara, A. Takatsuki, H. Itoh, N. Shimamoto and K. Kinosita, Jr., *Nature*, 2001, **409**, 113–115.
21 Y. Rondelez, G. Tresset, K. V. Tabata, H. Arata, H. Fujita, S. Takeuchi and H. Noji, *Nat. Biotechnol.*, 2005, **23**, 361–365.
22 G. M. Skinner and K. Visscher, *Assay Drug Dev. Technol.*, 2004, **2**, 397–405.
23 Y. Rondelez, G. Tresset, T. Nakashima, Y. Kato-Yamada, H. Fujita, S. Takeuchi and H. Noji, *Nature*, 2005, **433**, 773–777.
24 P. J. Hung, P. J. Lee, P. Sabounchi, N. Aghdam, R. Lin and L. P. Lee, *Lab Chip*, 2005, **5**, 44–48.
25 K. R. King, S. Wang, D. Irimia, A. Jayaraman, M. Toner and M. L. Yarmush, *Lab Chip*, 2007, **7**, 77–85.
26 D. Di Carlo, K. H. Jeong and L. P. Lee, *Lab Chip*, 2003, **3**, 287–291.
27 T. C. Marentis, B. Kusler, G. G. Yaralioglu, S. Liu, E. O. Haeggstrom and B. T. Khuri-Yakub, *Ultrasound Med. Biol.*, 2005, **31**, 1265–1277.
28 U. Lehmann, C. Vandevyver, V. K. Parashar and M. A. Gijs, *Angew. Chem., Int. Ed.*, 2006, **45**, 3062–3067.
29 H. Lu, M. A. Schmidt and K. F. Jensen, *Lab Chip*, 2005, **5**, 23–29.
30 N. Ikeda, N. Tanaka, Y. Yanagida and T. Hatsuzawa, *Jpn. J. Appl. Phys.*, 2007, **46**, 6410–6414.
31 D. W. Lee and Y.-H. Cho, *Sens. Actuators, B*, 2007, **124**, 84–89.
32 D. Di Carlo, C. Ionescu-Zanetti, Y. Zhang, P. Hung and L. P. Lee, *Lab Chip*, 2005, **5**, 171–178.
33 A. Bhattacharyya and C. M. Klapperich, *Anal. Chem.*, 2006, **78**, 788–792.
34 X. Chen, D.-F. Cui, C.-C. Liu and H. Li, *J. Micromech. Microeng.*, 2007, **17**, 68–75.
35 D. C. Duffy, J. C. McDonald, O. J. A. Schueller and G. M. Whitesides, *Anal. Chem.*, 1998, **70**, 4974–4984.
36 A. Griebel, S. Rund, F. Schonfeld, W. Dorner, R. Konrad and S. Hardt, *Lab Chip*, 2004, **4**, 18–23.
37 Y. C. Wang, M. H. Choi and J. Han, *Anal. Chem.*, 2004, **76**, 4426–4431.
38 R. A. Monticello, E. Angov and W. S. Brusilow, *J. Bacteriol.*, 1992, **174**, 3370–3376.
39 K. Y. Hara, H. Noji, D. Bald, R. Yasuda, K. Kinosita, Jr. and M. Yoshida, *J. Biol. Chem.*, 2000, **275**, 14260–14263.
40 H. Noji, D. Bald, R. Yasuda, H. Itoh, M. Yoshida and K. Kinosita, Jr., *J. Biol. Chem.*, 2001, **276**, 25480–25486.
41 R. F. Ismagilov, A. D. Stroock, P. J. A. Kenis and G. Whitesides, *Appl. Phys. Lett.*, 2000, **76**, 2376.
42 A. E. Kamholz and P. Yager, *Biophys. J.*, 2001, **80**, 155–160.
43 F. Han, Y. Wang, C. E. Sims, M. Bachman, R. Chang, G. P. Li and N. L. Allbritton, *Anal. Chem.*, 2003, **75**, 3688–3696.
44 H. He, D. C. Chang and Y.-K. Lee, *Bioelectrochemistry*, 2007, **70**, 363–368.

Supplementary Material (ESI) for Lab on a Chip
This journal is © The Royal Society of Chemistry 2008

Supplementary information

1. Cell lysis evaluation by SDS-PAGE

The cell lysis condition was evaluated quantitatively by absorptiometry at 280 nm (OD_{280}), as described in the main text. However, the measured absorbance is attributed to all proteins, including contaminants. We additionally electrophoresed several protein solutions used in our experiment, as shown in Fig. S1. For comparative purposes, a solution flowed in the cell lysis chamber with no applied voltage in lane 1. Lysates for lanes 2 and 3 were prepared by the on-chip cell lysis, with applied voltages of 150 V (60 kV/cm) and 250 V (100 kV/cm), respectively. In the cell lysis, other parameters were as follows: flow rate for the cell lysis chamber (3 μL/min), duty (0.01%), and pulse width (50 μs), which was used to examine the diffusion phenomenon in the assay channel. Lanes 4 to 9 were obtained by diluting an F_1 solution purified off-chip conventionally. The initial F_1 concentration of 2.5 μM was adjusted to 10~100 nM. The result indicates that F_1 molecules consisting of α, β, γ-subunits were predominantly detected in lanes 2 and 3, even though other contaminated proteins were slightly observed in the same lanes. Focusing on these F_1 components, F_1 concentrations in lysates can be approximately estimated as 30 nM and 70 nM for lanes 2 and 3, respectively.

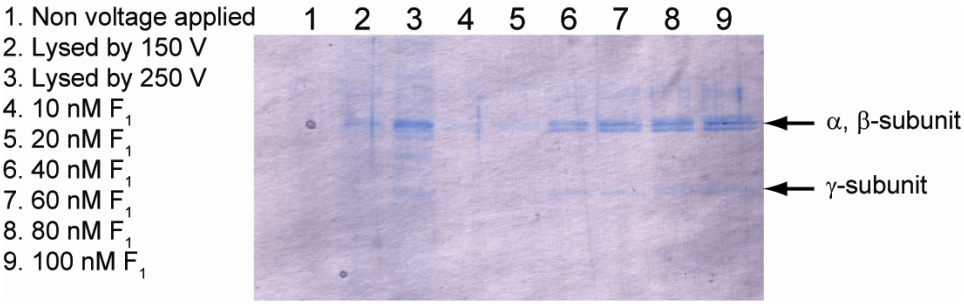

Fig. S1 Proteins separated by SDS-PAGE. The inset indicates the sample preparation for each lane.

2. The on-chip rotation assay using pseudo lysates

Unstable flow caused by missed operation of the SMM may disturb the concentration gradients of lysates, resulting in the failure to optimize the single molecule assay condition. To confirm the diffusion phenomena discussed in the main text, we imitated the diffusion using pseudo lysates in a Y-shaped channel. Lysates were prepared by mixing F_1 purified off-chip and contaminated proteins obtained by the sonication of *E. coli* without F_1 expression. Then the pseudo lysates were diluted to have the same OD_{280} as obtained in Fig. 3b: OD_{280}=0.16 for 150 V (60 kV/cm), 0.32 for 250 V (100 kV/cm), and 11.5 for sonication. The same assay protocol shown in Table 1 was performed by replacing the "cell solution" by the pseudo lysate. Densities of the rotating microspheres were plotted, as shown in Fig. S2, in which the same coloured symbols as used in Fig. 6 were used for comparison. The density was maximized at the similar position in the *y*-direction, as measured in the sequential assay in the SMM (Fig. 6b). The results support that lysate concentration is optimized for the single molecule assay.

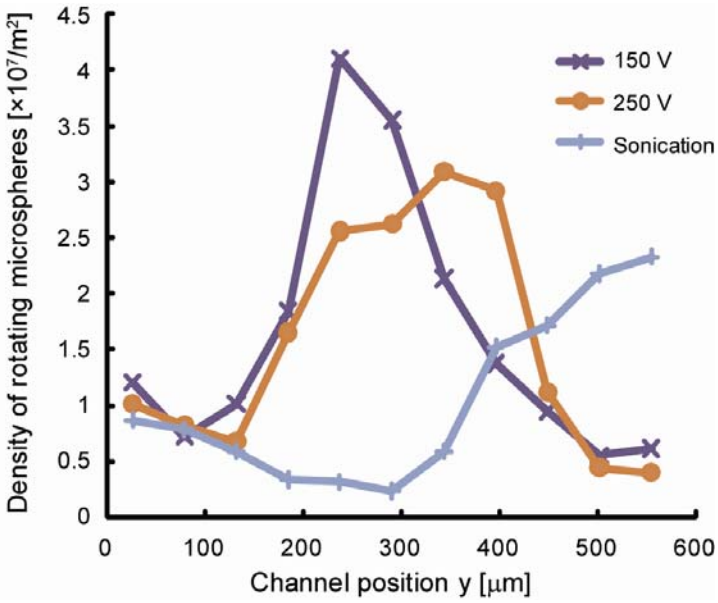

Fig. S2 Density distribution of rotating microspheres in the *y*-direction measured by assays using pseudo lysates.